ELSEVIER

Journal of Power Sources 55 (1995) 259–262

JOURNAL OF POWER SOURCES

Short Communication

Solid-state photovoltaic power and battery unit

R. Koksbang, J. Barker

Valence Technology, Inc., 301 Conestoga Way, Henderson, NV 89015, USA

Received 20 January 1995; accepted 9 February 1995

Abstract

The feasibility of an integrated battery/solar module system is demonstrated using a rechargeable lithium battery and a commercially available polycrystalline silicon solar module. The solar module was parallel connected to a prismatic 500 mAh battery and a constant resistance load. This arrangement was subsequently tested under conditions which simulated daylight and night conditions. The combined system was cycled 20 times without severe degradation of the battery or solar module performance.

Keywords: Lithium; Rechargeable lithium batteries; Solar cells; Polymers; Photovoltaic systems

1. Introduction

Conventional photovoltaic (PV) systems are normally equipped with batteries for charge-storage purposes. Certainly this is the case for normal stand-alone PV systems which are expected to be the dominant PV application in the immediate future [1,2]. Only a limited number of batteries have been considered by the PV industry to offer the necessary combination of properties required for such applications. For instance, the batteries must be relatively maintenance free, exhibit low self-discharge and demonstrate relatively long charge/discharge cycle life. Furthermore, the batteries must also be able to perform adequately over a wide range of operating temperatures [3].

The batteries used in most applications are of the lead/acid-type since these are considered by the industry to offer a stable and reliable component proved by many years of satisfactory performance at, for example, power utilities, remote telecommunications sites and at other PV installations. Although these batteries possess good cycling properties, the volumetric and gravimetric energy densities are somewhat low when compared with more advanced secondary battery systems. Unfortunately, in spite of many significant advances having been made in improving the performance of PV devices (i.e. solar energy conversion efficiency, light soak stability) the industry has been relatively slow to incorporate the corresponding improvements in charge-storage capability [4]. Significant advances have been made in improving substantially such properties as the energy density and cycle life of these new battery systems. One of the most advanced batteries to recently near commercialization is the lithium metal–polymer electrolyte system which has been described in detail in several recent publications [5,6].

The particular battery system used in this study incorporates a composite V_6O_{13} cathode as the electrochemically active material. This system has been demonstrated to possess excellent rechargeability together with volumetric and gravimetric energy densities far in excess of either lead/acid or Ni–Cd technologies and it can also operate successfully over a wide temperature range [5,6]. The physical properties of the electrodes and electrolyte mean the cells can be fabricated in many desirable shapes and sizes. This will allow the battery based on this technology to be relatively easily incorporated into existing PV systems. A further exciting prospect is the possibility of manufacturing combined PV power and battery systems within a single stand-alone unit. Of particular interest may be the fabrication of truly thin-film laminations by combination of this battery technology with the state-of-the-art thin-film solar cells based on amorphous Si [1], CdTe [7] or $CuInSe_2$ [8].

SSDI 0378-7753(95)02197-O

2. Experimental

The battery laminate was made as described elsewhere [5,6], using V_6O_{13} as the active cathode material, metallic lithium foil (75 μm thick) as the anode, and a polymeric solid electrolyte as both the electrode separator and as the binder in the composite cathode. The electrolyte was prepared by radiation induced polymerization of acrylate precursors and was plasticized with propylene carbonate (PC) to enhance the ionic conductivity [9,10]. The electrolyte salt used in these particular experiments was $LiAsF_6$.

Prismatic batteries were constructed by parallel connection of individual cells, and encapsulating the battery stack in a flexible encapsulation by vacuum sealing [6].

For the tests, a sun-simulator system was used, which incorporated two 650 W ELH lamps supplied by General Electric. Both the solar intensity and the irradiance spectrum of the lamps match those of natural sunlight closely. The lamps were placed at a distance of 45 cm from the test plane and at an angle of 70° from the horizontal test plane, providing an irradiance of 100 mW/cm^2.

The solar cell panel used was a Solarex MSX-005. This panel comprises 8 series connected polycrystalline silicon cells. The measured current–voltage (I–V) characteristics supplied by the manufacturers indicate an approximate open-circuit voltage V_{oc} of 0.58 V per cell and a short-circuit current I_{sc} of 160 mA. Under optimized load conditions and 100 mW/cm^2 solar irradiation the panel produces a peak power which corresponds to a current of between 130 and 150 mA at a nominal load voltage of 3.3 V [11].

3. Results and discussion

PV systems in their simplest form normally possess three components – module, battery and load – all connected in parallel. Dependent on the solar irradiance available the battery current may be positive (during battery charging) or negative (during battery discharge). In more complicated arrangements suitable for commercial application, voltage regulators are included, which minimize overcharge and overdischarge conditions which may be harmful to the battery.

For good performance of the combined PV power and battery unit the proper matching of the module and load/battery must be determined by considering the maximum power curve of the PV module. A schematic representation of the I–V characteristics of a typical solar cell under illumination is shown in Fig. 1 [4]. The precise operating point is determined by the intersection of the solar module I–V characteristics and the load (resistive) I–V characteristics. For a truly resistive load of the fixed resistance, R, the operating point will be determined by the intersection of the I–V characteristics and the load. The power delivered to the load only depends on the value of R. If the value of R is small, the module will behave essentially as a constant-current source (as indicated in Fig. 1), generating a constant current to the load, which for a good solar module will approach the short-circuit current value. At this operation point the output voltage will be somewhat short of the V_{oc} value for the module. If the value of R is relatively high, the module will operate as a constant-voltage source (again indicated in Fig. 1) where the output voltage will approach the V_{oc} value, but with a substantially lower current than defined by I_{sc}.

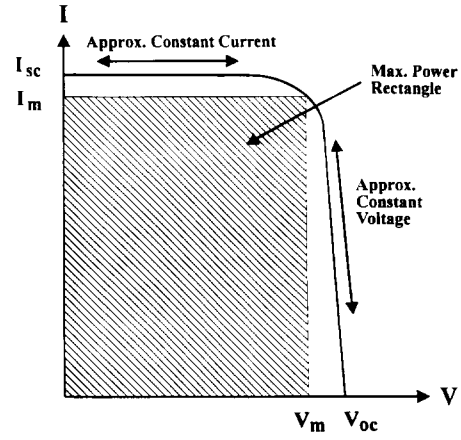

Fig. 1. Schematic representation of the current–voltage characteristics of a solar cell under illumination [4].

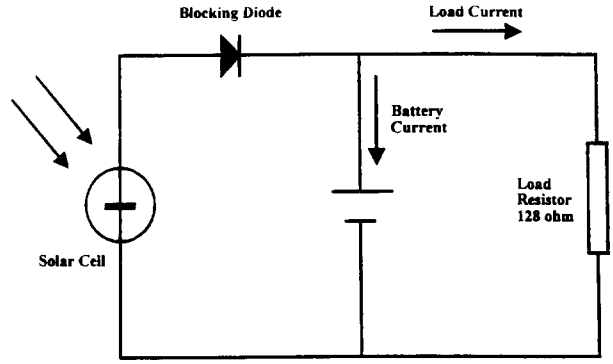

Fig. 2. Electronic circuit for test of the combined battery and solar cell panel unit.

In the system used in this study the total load resistance (battery and load resistor) were selected to be relatively large and hence the solar module will behave essentially as a constant-voltage source. Thus the module acts as a constant-voltage charging device for the Li–V_6O_{13} battery. The test circuit used is depicted in Fig. 2. A constant load of 128 Ω is applied to the battery and solar panel continuously to simulate the power requirements of a possible application. This load corresponds to a current of about 25 mA, i.e., a current some distance from the rated I_{sc}. The irradiance of the

lamps, recharge the battery at a constant potential of about 3 V for 12 h every 24 h. The solar panel delivers a total current of 50 mA under the applied irradiation conditions, of which about 25 mA is dissipated in the resistor and the rest is used to recharge the battery. The diode in the circuit is primarily used to prevent discharge of the battery through the solar panel circuit, as it will only allow current to flow in one direction.

Cycling of battery cells using V_6O_{13} as the active cathode material has been shown previously [5]. A typical voltage curve versus capacity is shown in Fig. 3, for both discharge and charge. It can be seen from inspection of the Figure that the cell voltage typically varies between ~3 V versus Li in the fully charged state and 1.8–2.1 V versus Li in the discharge condition. The thermodynamic open-circuit voltage of unlithiated V_6O_{13} is close to 2.8 V versus Li [12], such that the charge potential applied by the solar panel is somewhat higher than required. However, no degradation of the battery performance is expected at charge potentials below 3.5 V versus Li [13].

The solar simulation corresponds to 12 h of light and 12 h of darkness, with approximately half of the current used to sustain the load in the light period, and about 25 mA used to charge the battery. Under these conditions, a battery of a minimum capacity of 300 mAh is required. Since cycling under 100% depth-of-discharge (DOD) conditions is considered to be unlikely under real-life conditions, the battery was designed as a nominal 500 mAh battery, in which a typical DOD would be about 60% of the nominal capacity.

Due to the physical dimensions and the electrical characteristics of the solar cell panel (Table 1), it proved to be unnecessary to optimize the physical dimensions of the combined unit. It should be noted that in an optimized system in which the battery becomes an integral part of the solar module the volumetric energy density should be higher.

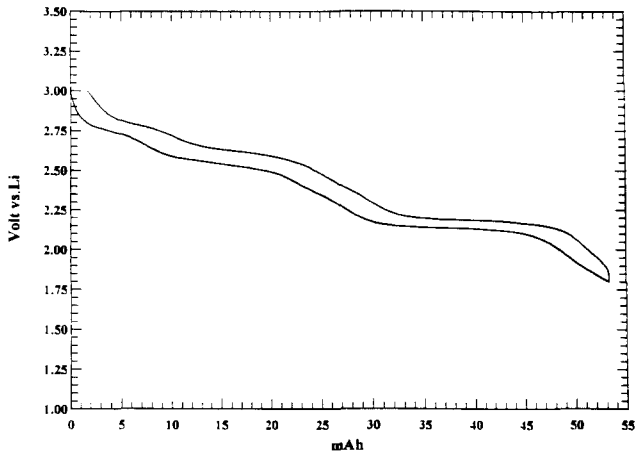

Fig. 3. Typical discharge/charge curve for a V_6O_{13}/Li battery.

Table 1
Solar panel and battery component dimensions

	Solar cell	Solar cell panel	Battery components	Complete battery
Width (mm)	67	79	40	60
Length (mm)	114	148	80	118
Thickness (mm)	3	10	3	4

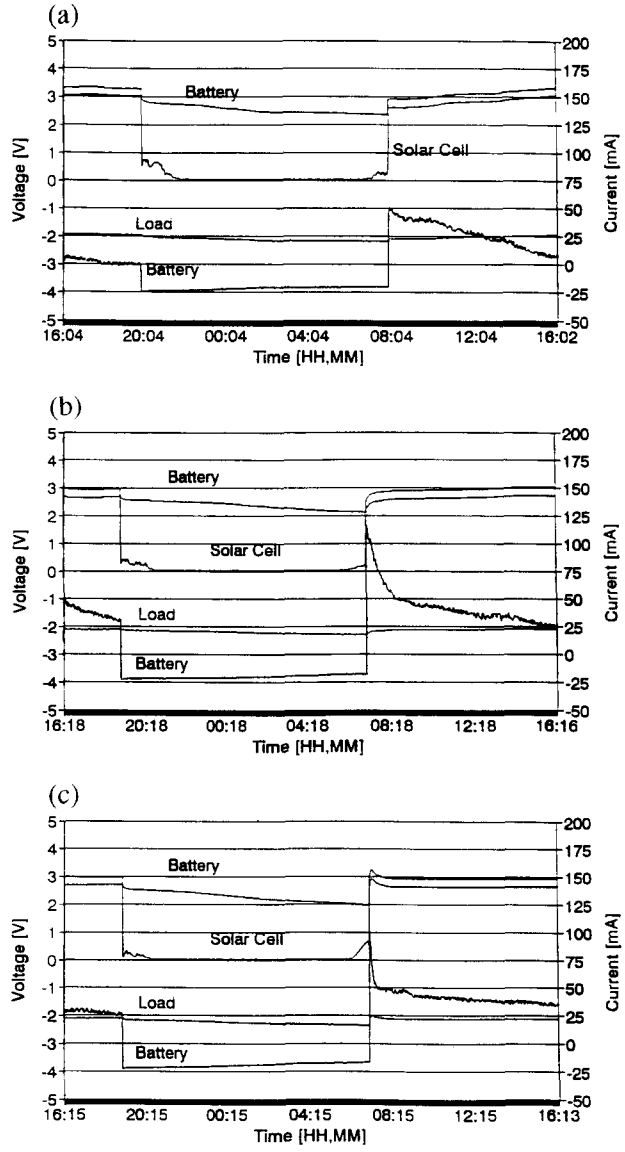

Fig. 4. Voltage (left axis) and current (right axis) characteristics of battery and solar cell during cycling, as function of time. The legends in the Figure indicate the origin of the curves. Note that the load current is the total current used to charge the battery and sustain the current drain caused by the resistor. The two upper traces are potentials while the two lower traces are current. (a) Cycle 2, (b) cycle 10, and (c) cycle 20.

The results of a typical test described in the previous sections, are given in Fig. 4(a)–(c), which shows characteristic discharge and charge data for both the battery

and for the complete system for cycle 2, 10 and 20. Fig. 4 shows the battery and solar cell panel potentials (upper two traces) and the load and total current (lower traces) passed through the battery. During the initial discharge across a 128 Ω resistor, a current of approximately 25 mA is delivered by the battery for a period of 12 h. The discharged capacity corresponds to about 60% of the nominal capacity. During this period (a dark period), the solar cell is inactive and the associated potential and current are zero. The battery potential is declining gradually from approximately 3 to about 2.4 V, as expected, considering the 60% DOD and with reference to Fig. 3.

The load current is almost constant 25 mA during both charge and discharge periods. Similarly, the battery current is reasonably constant around 25 mA during discharge, while it raises to about 50 mA during the initial charge, and then gradually decays to close to zero towards the end of charge. The low final current indicates that the battery is close to fully charged at the end of the 12 h potentiostatic charge period. However, the current is decaying linearly rather than exponentially as expected. The exponential decay is developing during progressive cycling, simultaneously with the appearance and gradual increase in a current spike when charge is initiated in each cycle. After 20 cycles, the current spike reaches a value of about 100 mA, i.e. twice the initial starting charge current. Neither of these observations can be explained at present, but are presumably related to the constant-potential recharge method applied by the solar cell device.

Comparison of the voltage curves of the battery and the solar cell during charge reveal that some energy is lost due to an *IR* drop in the battery. However, the amount is relatively small and seems to be unchanged after 20 cycles.

The battery potential gradually decreases during cycling. The initial 3 V recharge potential, and corresponding 2.4 V discharge potential, decrease to about 2.8 and 2.0 V after 20 cycles indicating that the recharge is somewhat inefficient. Although the observations indicate that some changes take place during cycling under potentiostatic conditions, no severe damage to the battery is observed.

4. Conclusions

A combined battery/solar module system has been tested under simulated solar irradiance conditions. The solar module was designed to provide sufficient energy and power during the light periods, to simultaneously recharge the battery and sustain the current on the resistive load. The capacity of the battery was carefully chosen so as to be sufficient to drive the load during the dark periods.

The feasibility of a combined lithium battery/solar module system has been demonstrated according to these requirements. The combined system was cycled 20 times without severe degradation of the battery performance, before the test was terminated.

By properly designing and matching the two components, it is possible to construct an integrated battery/solar module unit, in which the battery volume is of approximately the same size as the solar module. Furthermore, the battery is easily contained within the volume of the panels currently used to house the type of solar modules used in this work. Furthermore, the weight of the lithium battery is significantly lower than the weights of commonly used rechargeable batteries and thus contribute less to the total overall weight of the unit.

References

[1] K. Zweibel, *Harnessing Solar Power, The Photovoltaic Challenge*, Plenum, New York, 1991.
[2] A.L. Fahrenbruch and R.H. Bube, *Fundamentals of Solar Cells: Photovoltaic Solar Energy Conversion*, Academic Press, New York, 1983.
[3] F. Lasnier and T.G. Ang, *Photovoltaic Engineering Handbook*, IOP Publishing, Bristol, 1990.
[4] S.M. Sze, *Physics of Semiconductor Devices*, Wiley, New York 2nd edn., 1981, p. 795.
[5] R. Koksbang, I.I. Olsen and D. Shackle, *Solid State Ionics, 69* (1994) 320.
[6] R. Koksbang, F. Flemming, I.I. Olsen, P.E. Tønder, K. Brøndum, M. Consigny, K.P. Petersen and S. Yde-Andersen, in K.M. Abraham, M. Solomon (eds.), *Primary and Secondary Lithium Batteries*, The Electrochemical Society, Pennington, NJ, USA, Vol. 91-3, 1991, p. 157.
[7] (a) J. Barker, S.P. Binns, D.R. Johnson, R.J. Marshall, S. Oktik, M.E. Ozsan, M.H. Patterson, S.J. Ransome, S. Roberts, M. Sadeghi, J. Sherborne, A.K. Turner and J.M. Woodcock, *Int. J. Solar Energy, 12* (1992) 79; (b) D. Bonnet, *Int. J. Solar Energy, 12* (1991) 1.
[8] K. Mitchell, G.A. Pollock and A.V. Mason, *Proc. 20th IEEE Photovoltaic Conf.*, Institute of Electric and Electronic Engineers, New York, NY, 1988, p. 1542.
[9] I.I. Olsen, *Ph.D. Thesis*, University of Odense, Denmark, 1994.
[10] I.I. Olsen and R. Koksbang, Ext. Abstr., *Fall Meet. The Electrochemical Society, Miami, FL, USA, 1994*, Vol. 94-2, Abstr. No. 121, p. 190.
[11] *Solarex Data Sheet No. 6078-1, Special Photovoltaic Products for OEM Power Applications*, Solarex Corporation, 1990.
[12] K. West, B. Zachau-Christiansen and T. Jacobsen, *Electrochim. Acta, 28* (1983) 1829.
[13] R. Koksbang, F. Flemming, I.I. Olsen, P.E. Tønder, T.P. Andersen and S. Yde-Andersen, *Ext. Abstr., 180th Meet. The Electrochemical Society, Phoenix, AZ, USA, 13–18 Oct. 1991*, Vol. 91-2, Abstr. No. 692, p. 1031.